Microstructural Design of High-Strength Aluminum Alloys

J.F. Nie and B.C. Muddle
Department of Materials Engineering
Monash University, Clayton, Victoria, Australia 3168
Contact e-mail: barry.muddle@eng.monash.edu.au

(Submitted 27 January 1998; in revised form 22 June 1998)

A summary is presented of recent attempts to model the effects of precipitate shape, orientation, and distribution on yield strength and age-hardening response, using appropriate versions of the Orowan equation and models of precipitation strengthening developed for Al alloys containing a single uniform distribution of rationally oriented plate- or rod-shaped precipitates, which are either shearable or shear resistant. It is demonstrated that these models of particle strengthening are capable of predictions that are in excellent quantitative agreement with experimental observations that high tensile yield strength is associated with microstructures containing a high density of intrinsically strong, plate-shaped precipitates with $\{111\}_\alpha$ or $\{100\}_\alpha$ habit planes and large aspect ratio. The authors predict that further improvement in the strength of existing Al alloys might be achieved by increasing the number density and/or aspect ratio of rationally oriented precipitate plates.

1. Introduction

A common feature of high-strength (tensile yield strength ≥450 MPa) and ultrahigh-strength (yield strength ≥700 MPa) Al alloys is that maximum strength and hardness are achieved through precipitation hardening involving predominantly plate-shaped precipitates formed on rational habit planes, $\{111\}_\alpha$ and $\{100\}_\alpha$, in an α-Al matrix [94Mud, 95Pol] (Fig. 1). However, there is currently little detailed quantitative understanding of the strengthening mechanisms operative and of the relationship between the form and distribution of the strengthening intermediate precipitate phases and the observed yield strength. The development of high-strength Al alloys remains largely empirical, and there is a need for an improved theoretical basis for alloy design [93Hor].

It is the purpose of this article to review selected results of the modeling of the effects of precipitate shape, orientation, and distribution on yield strength and the age-hardening re-

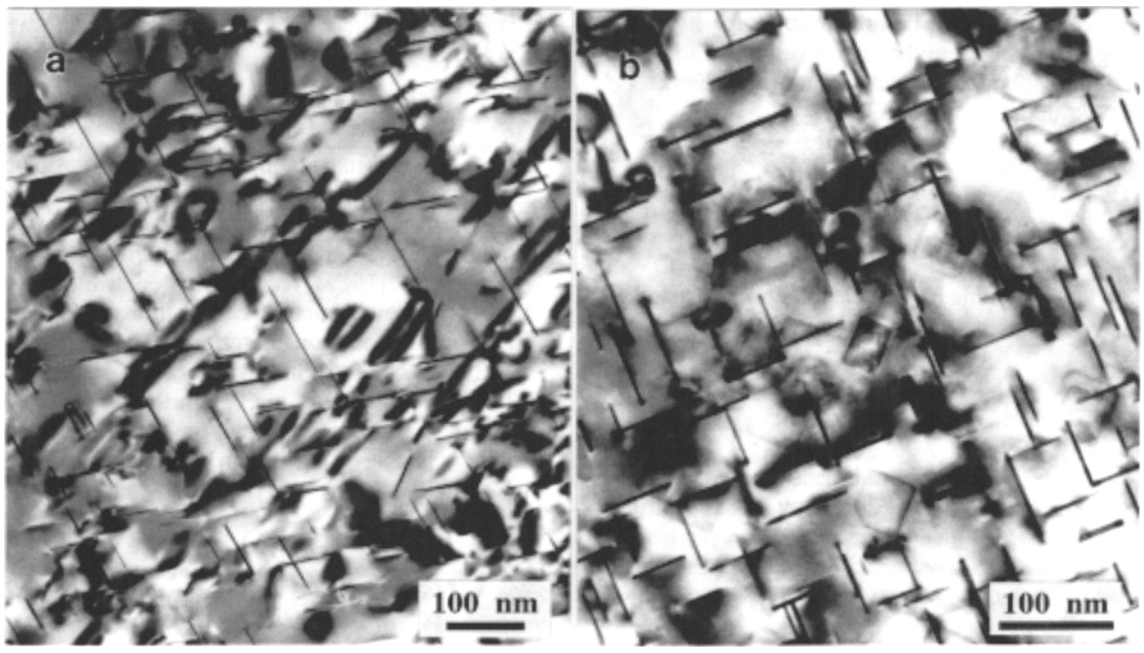

Fig. 1 Transmission electron micrographs showing **(a)** $\{111\}_\alpha$ precipitate plates of T_1 phase in Al-2.86Cu-2.05Li-0.12Zr alloy (AA2090-T8E41: cold worked 6% and aged 24 h at 163 °C) reversion heat treated for 120 s at 270 °C and **(b)** $\{100\}_\alpha$ precipitate plates of θ′ phase in Al-4Cu-0.05Sn alloy aged 3 h at 200 °C.

sponse, using appropriate versions of the Orowan equation [48Oro] and models of precipitation strengthening developed for rationally oriented precipitate plates and rods. The work seeks to identify those aspects of metastable phase equilibria and the resulting microstructural parameters that are important in optimizing precipitation hardening or dispersion strengthening.

2. Microstructures Containing Spherical Particles

2.1 Shearable Precipitates

Shearable precipitates can impede the movement of gliding dislocations through a variety of dislocation/particle interaction mechanisms, including those described as interfacial (chemical) strengthening, coherency strengthening, stacking-fault strengthening, modulus strengthening, and order strengthening [86Ard, 89Emb, 93Rep, 97Nem]. For each such proposed mechanism of strengthening, the contribution of the shearable precipitates to the critical resolved shear stress (CRSS) of an alloy can be represented generally by an equation of the form [63Fri]:

$$\Delta\tau = \left(\frac{2}{\mathbf{b}\sqrt{\Gamma}}\right)\left(\frac{1}{L_P}\right)\left(\frac{F}{2}\right)^{3/2} \quad \text{(Eq 1)}$$

where $\Delta\tau$ is the increment in CRSS, **b** is the Burgers vector of the slip dislocations, Γ is the dislocation line tension in the matrix phase, L_P is the mean planar center-to-center interprecipitate spacing, and force F is a measure of the resistance of the precipitates to dislocation shearing. For the purposes of this article, it is convenient to restrict discussion to two of the more important mechanisms contributing to strength: interfacial strengthening and order strengthening. Assuming a square array distribution of spherical particles of uniform diameter d_t, Eq 1 can be rewritten in the form:

$$\Delta\tau = \frac{1.922}{d_t}\left(\frac{\mathbf{b}f}{\Gamma}\right)^{1/2}\gamma_i^{3/2} \quad \text{(Eq 2)}$$

for interfacial strengthening [97Nie], and for order strengthening [85Ard]:

$$\Delta\tau = \left(\frac{\gamma_{apb}}{2\mathbf{b}}\right)\left(\sqrt{\frac{3\pi^2\gamma_{apb}f d_t}{64\Gamma}} - f\right) \quad \text{(Eq 3)}$$

where f is the volume fraction of particles, γ_i is the specific interfacial energy between precipitate and matrix phases, and γ_{apb} is the specific antiphase boundary energy on the slip plane of the precipitate phase.

2.2 Shear-Resistant Precipitates

If it is assumed that a dispersion of spherical particles is distributed uniformly over the slip plane of the matrix phase, then the Orowan increment in CRSS produced by the need for dislocations to bypass these particles is given as [48Oro, 86Ard, 89Emb]:

$$\Delta\tau = \left\{\frac{G\mathbf{b}}{2\pi\sqrt{1-\nu}}\right\}\left\{\frac{1}{\lambda}\right\}\left\{\ln\frac{\pi d_t}{4r_0}\right\} \quad \text{(Eq 4)}$$

where G is the shear modulus of the Al matrix phase, ν is Poisson's ratio, r_0 is the core radius of dislocations, and the effective planar interprecipitate spacing is given as:

$$\lambda = \left(C\sqrt{\frac{\pi}{6f}} - \frac{\pi}{4}\right)d_t \quad \text{(Eq 5)}$$

where constant C takes values of 1, 1.075, and 1.23 for square, triangular, and random arrays of precipitates, respectively [73Kel].

2.3 Experimental Evaluation

It has been well documented that coherent, spherical δ' precipitates (Al_3Li) are sheared during deformation of underaged Al-Li alloys [93Rep] and that the yield strength of underaged alloys can be accounted for quantitatively using the model of order strengthening [88Hua, 92Ger, 94Jeo, 95Sch] defined in Eq 3. It has also been reported [92Ger] that maximum strength of precipitation-hardened Al-Li alloys corresponds to an average particle diameter of ~40 nm, above which a transition from dislocation shearing to dislocation looping occurs. However, the strengthening models for underaged and overaged samples have not been combined with data on precipitation kinetics to predict the age-hardening response of Al-Li alloys.

The variation in precipitate volume fraction during isothermal aging can be represented by a form of the Kolmogorov-Johnson-Mehl-Avrami (KJMA) relationship [37Kol, 39Avr, 39Joh]:

$$f = f_m\left(1 - \exp\left(-kt^n\right)\right) \quad \text{(Eq 6)}$$

where f_m is the maximum volume fraction of precipitates at a given aging temperature, f is the volume fraction of precipitates at a given time t, k is a constant that depends on the nucleation and growth rates, and the time exponent n may take values in the range 0.5 to 4 [75Chr] for diffusion-controlled precipitation. In the case of homogeneous precipitation of δ' phase in Al-Li alloys, the kinetics of precipitation can be well predicted when n is 0.8 [97Nob] and k is in the range 0.001 to 0.004 [86Cas, 88Hua, 92Ger, 92Sch, 92Tri, 94Jeo, 95Sch, 96Jeo].

The growth of spherical precipitates during the initial stages of isothermal aging can be modeled using an equation of the form [91Wag]:

$$\bar{d}_t = 2\sqrt{2}\left(\frac{C_0 - C_e}{C_p - C_e}\right)^{1/2}(D_v t)^{1/2} = f(T)\,t^{1/2} \quad \text{(Eq 7)}$$

where $\bar{d}_t$ is the average diameter of spherical precipitates at time t, C_0 is the alloy composition, C_e is the equilibrium solid solubility of solute in the matrix phase, C_p is the composition

of the precipitate phase, D_v is the volume diffusion coefficient of the solute element, and T is the aging temperature (in Kelvin). Once the maximum precipitate volume fraction is established, the coarsening rate of the precipitates can be described by the Lifshitz-Slyozov-Wagner (LSW) equation [61Lif, 61Wag]:

$$\bar{d}_t = \left(\frac{8 D_v \gamma_i C_e V_m}{9RT} t \right)^{1/3} = f(T)\, t^{1/3} \qquad \text{(Eq 8)}$$

where V_m is molar volume of the precipitate, and R is the gas constant. Because growth and coarsening of the precipitates occur simultaneously during the initial stages of precipitation, and the observed growth rate of δ′ precipitates in Al-Li binary alloys during isothermal aging matches well with that predicted by Eq 8 [96Jeo, 97Nob], Eq 8 is used here to establish the variation in the average diameter of precipitate particles with time.

Combining Eq 6 and 8, the variation in the number density, N_v, of precipitates per unit volume as a function of time is given as [97Nie]:

$$N_v = \frac{6f}{\pi \bar{d}_t^3} = \frac{1.91 f_m (1 - \exp(-kt^n))}{(f(T))^3 t} \qquad \text{(Eq 9)}$$

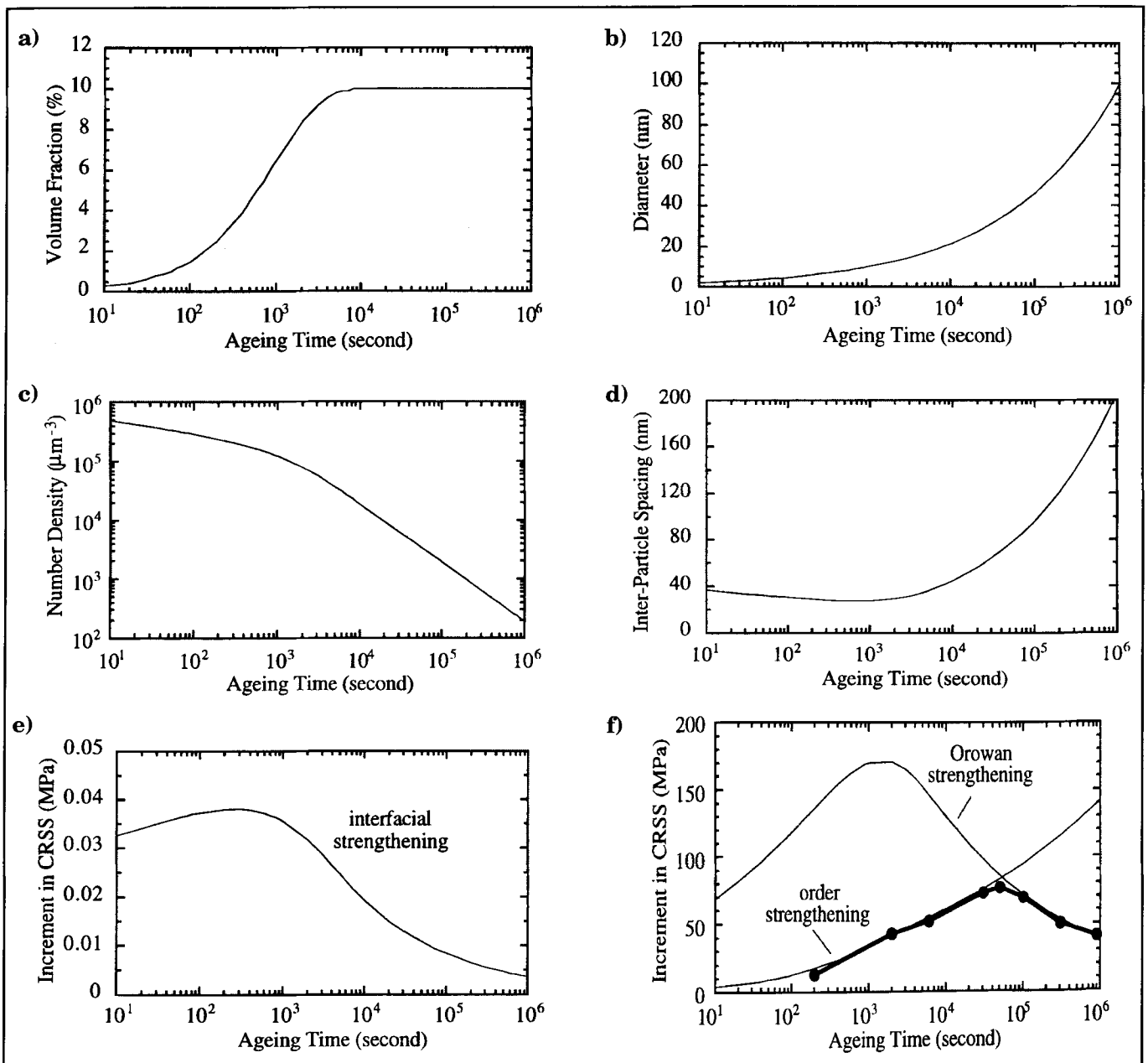

Fig. 2 Variation with aging time of (**a**) volume fraction, (**b**) particle diameter, (**c**) particle number density, (**d**) effective interparticle spacing, (**e**) increment in CRSS arising from interfacial strengthening, and (**f**) increment in CRSS arising from order strengthening and Orowan strengthening. The Al-2.3Li alloy was aged at 200 °C, and solid circles in (**f**) represent measured increments in CRSS [92Ger].

Substituting Eq 6 and 8 into Eq 2 to 4 allows the variation of the increments in CRSS with aging time to be calculated for the mechanisms of interfacial strengthening, order strengthening, and Orowan strengthening, respectively.

For precipitation of δ′ phase in an Al-2.3Li (wt.%) binary alloy, the variations as a function of aging time at 200 °C in the volume fraction, particle diameter, and number density per unit volume, and effective interparticle spacing are shown in Fig. 2(a) to (d), respectively. The increments in CRSS arising from interfacial and order strengthening and from Orowan hardening are plotted in Fig. 2(e) and (f), respectively. The data on the size and volume fraction of precipitates are taken from [92Ger], but the maximum volume fraction of δ′ precipitates has been limited to 0.1. The reported value of $f_m = 0.16$ appears to overestimate the volume fraction of δ′ phase, because calculations based on the established Al-Al_3Li (δ′) metastable phase diagram [88Kha] yield a maximum of 0.11. In addition, the maximum volume fraction of δ′ precipitates has been measured to be less than 0.1 in most studies of Al-Li alloys with similar compositions and aging treatments. Other data used in the calculations for Fig. 2 are: $k = 0.00416$ (determined from measured data on precipitate volume fraction), $G = 25$ GPa [90Met], $b = 0.286$ nm, $\gamma_{apb} = 0.165$ J/m^2 for δ′ phase on $\{111\}_{\delta'}$ planes [92Ger], $\gamma_i = 0.014$ J/m^2 [84Bau]. It has been assumed that the δ′ particles are randomly distributed, and that the dislocation line tension Γ is given by [92Ger]:

$$\Gamma = \frac{Gb^2}{2\pi} \ln \sqrt{\frac{d_t^2}{2b^2 f}} \qquad \text{(Eq 10)}$$

Figure 2(e) shows that the contribution of interfacial strengthening to CRSS is negligible, while Fig. 2(f) shows that increments in CRSS observed for underaged samples appear to be well predicted by the order-strengthening model. The maximum strength of the alloy corresponds to a particle size of approximately 40 nm diameter, and there appears to be a transition from dislocation shearing to dislocation looping at this critical particle size, which is in excellent agreement with experimental observations [92Ger]. For overaged samples, the increments in CRSS are equivalent to those predicted by the Orowan equation.

An interesting observation is that, seen in isolation, the increment in Orowan strengthening rises to a maximum with increasing aging time and then declines and that the maximum in the Orowan increment corresponds approximately to the minimum value of the effective interparticle spacing.

Table 1 Equations Defining Increments in CRSS due to Interfacial Strengthening for Al Alloys Containing Regular Triangular Arrays of Shearable Precipitates

Increment in CRSS for interfacial strengthening	Precipitate form
$\Delta\tau = \frac{1.211\, d_t}{t_t^2}\left(\frac{bf}{\Gamma}\right)^{1/2}\gamma_i^{3/2}$	$\{111\}_\alpha$ plates
$\Delta\tau = \frac{0.908\, d_t}{t_t^2}\left(\frac{bf}{\Gamma}\right)^{1/2}\gamma_i^{3/2}$	$\{100\}_\alpha$ plates
$\Delta\tau = \frac{1.110}{d_t}\left(\frac{bf}{\Gamma}\right)^{1/2}\gamma_i^{3/2}$	$\langle 100\rangle_\alpha$ rods

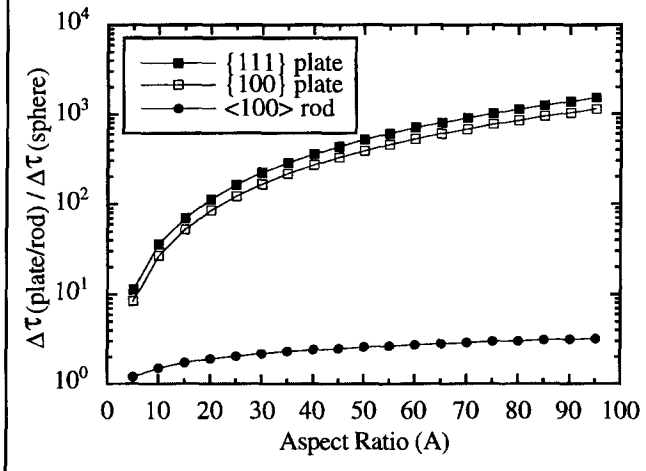

Fig. 3 Variation of ratio Δτ(plate/rod)/Δτ(sphere) with aspect ratio for $\{111\}_\alpha$ and $\{100\}_\alpha$ precipitate plates and $\langle 100\rangle_\alpha$ precipitate rods, calculated assuming interfacial strengthening of sheared particles.

3. Microstructures with Shearable Precipitate Plates

3.1 Theoretical Modeling

The results of geometric models developed [97Nie] to account for the contribution of interfacial strengthening to CRSS for Al alloys containing rationally oriented precipitate plates or rods are presented in Table 1. These equations have been derived assuming that there is continuity of the slip plane between matrix and precipitate and that the Burgers vector of the dislocations is identical in the two phases. They are based on an ideal regular triangular array of particles in the slip plane. Details of the models are presented in [97Nie].

For a given value of dislocation line tension, the variations in the ratio Δτ(plate/rod)/Δτ(sphere) with plate/rod aspect ratio for various forms of particle are shown in Fig. 3. Unlike the results for spherical particles, it is evident that the contribution due to interfacial strengthening may become significant when particles take, in particular, a plate-shaped form. For identical volume fractions and number densities of precipitates per unit volume, the yield stress increments produced by $\{111\}_\alpha$ and $\{100\}_\alpha$ precipitate plates are orders of magnitude larger than those produced by $\langle 100\rangle_\alpha$ precipitate rods and by spherical particles. The increments in CRSS produced by $\{111\}_\alpha$ and $\{100\}_\alpha$ plates increase substantially with an increase in plate aspect ratio and are up to three orders of magnitude larger than that produced by spheres, when the plate aspect ratio is in the range of 5-to-1 to 95-to-1. Interfacial strengthening can thus

potentially be a major strengthening mechanism in Al alloys containing rationally oriented, shearable precipitate plates of large aspect ratio.

3.2 Experimental Evaluation

The capability of the interfacial strengthening model has been examined using experimental data [87Hua] for the scale and distribution of precipitates in an Al-2.85Cu-2.3Li-0.12Zr (wt.%) alloy containing a uniform single distribution of $\{111\}_\alpha$ precipitate plates of T_1 phase (Al_2CuLi). The alloy was aged isothermally at 190 °C and then reversion heat treated for 60 s at 265 °C to dissolve δ′ and θ′ precipitates and to isolate the contribution of T_1 precipitate plates to yield strength [87Hua]. The measured variations in the dimensions of the T_1 plates, the precipitate volume fraction, and the increment in CRSS due to the precipitate distribution are plotted as a function of aging time at 190 °C in Fig. 4. It has been shown [88How, 97Nie] that T_1 precipitates are sheared in plastically deformed (3% strain) and fractured tensile samples in both underaged and overaged conditions, and thus it is appropriate to apply the model for interfacial strengthening to predict the contribution of the T_1 precipitates to the yield strength of the alloy. Assuming a value of $\gamma_i = 0.083$ J/m^2 (currently accepted values for specific precipitate/matrix interfacial energy vary in the range 0.01 to 0.1 J/m^2 for coherent precipitates), a Taylor factor of 3.331 [87Hua], $G = 25$ GPa, and $b = 0.286$ nm, the predicted increments in CRSS produced by the T_1 precipitates are in generally good agreement with values observed experimentally (Fig. 4d). It is important to emphasize, however, that the level of this agreement depends sensitively on the value selected for the energy of the precipitate-matrix interface created by the shearing dislocation and, at the present time, there is a lack of reliable data for γ_i. With this qualification, the interfacial strengthening model does appear capable of accounting plausibly for the yield strength and, more generally, the form of the age-hardening response of the alloy, when the effects of precipitate shape are included in the model.

The apparent success of this model, effectively over the entire aging regime, suggests that overaging is not necessarily accompanied by a transition from predominantly dislocation shearing to an Orowan looping mechanism. A comparison of predicted and observed increments in CRSS for overaged samples of an Al-2.86Cu-2.05Li-0.12Zr (wt.%) alloy (AA2090) is provided in Fig. 5 [97Nie]. For this independent set of measurements, the increments in CRSS predicted by the interfacial strengthening model are again in excellent agreement with observed values. Similar attempts to account for observed strength levels using alternative mechanisms of precipitation strengthening or Orowan hardening proved decidedly unsuccessful.

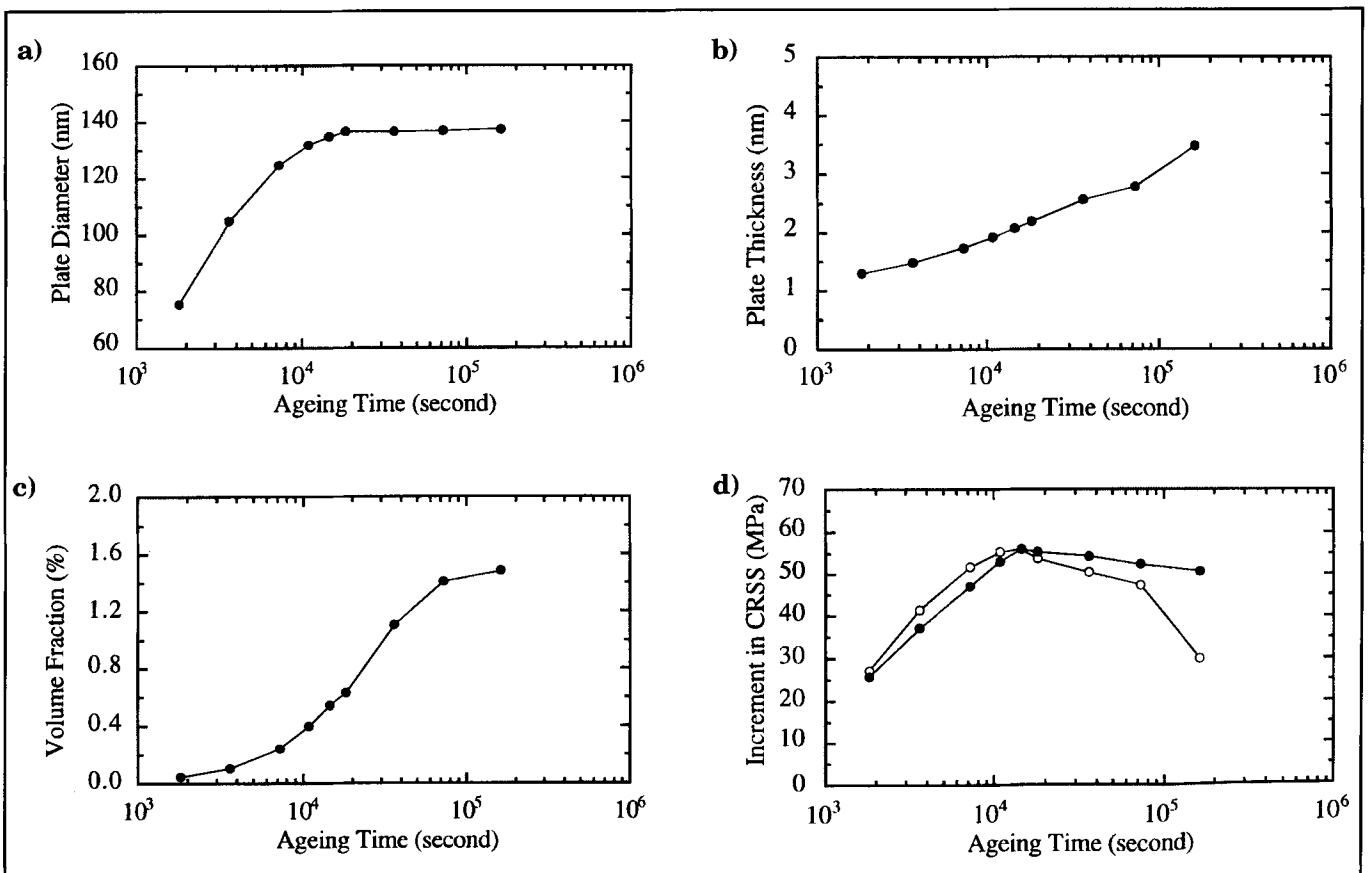

Fig. 4 Variation with aging time of (**a**) diameter, (**b**) thickness, (**c**) volume fraction of T_1 precipitates, and (**d**) increment in CRSS [87Hua]. The Al-2.85Cu-2.3Li-0.12Zr alloy was aged at 190 °C. Open circles represent values predicted using the interfacial strengthening model for sheared precipitate plates, and solid circles are values observed experimentally.

4. Microstructures Containing Shear-Resistant Plates

4.1 Theoretical Modeling

For aluminum alloys containing $\{111\}_\alpha$ and $\{100\}_\alpha$ precipitate plates, of uniform diameter d_t and thickness t_t, and $\langle 100\rangle_\alpha$ precipitate rods, of diameter d_t and length l_t, the appropriate versions of the Orowan equation [96Nie] are presented in Table 2. These equations are based on the assumption of a uniform periodic triangular array of precipitate particles intersecting the slip plane. Comparing similar precipitate volume fractions and number densities of precipitates per unit volume, the variations of the ratio $\Delta\tau$(plate/rod)/$\Delta\tau$(sphere) with plate/rod aspect ratio, for a precipitate volume fraction of 0.05, is shown in Fig. 6. To simplify comparison, the log terms in the strengthening equations are assumed to be identical, and the base microstructure is assumed to comprise spherical precipitates in a triangular array distribution on the slip plane of the matrix phase.

The Orowan increments in CRSS produced by $\{111\}_\alpha$ and $\{100\}_\alpha$ precipitate plates are invariably larger than those produced by $\langle 100\rangle_\alpha$ precipitate rods and spherical particles. The yield stress increment produced by $\{111\}_\alpha$ plates is larger than that arising from $\{100\}_\alpha$ plates and, for both precipitate orientations, the yield stress increment increases substantially with an increase in plate aspect ratio. There is a critical value of aspect ratio for each for which the effective interparticle spacing becomes zero and the plates form a continuous three-dimensional network. If the plates are assumed to remain shear resistant, then the Orowan increment becomes infinitely large.

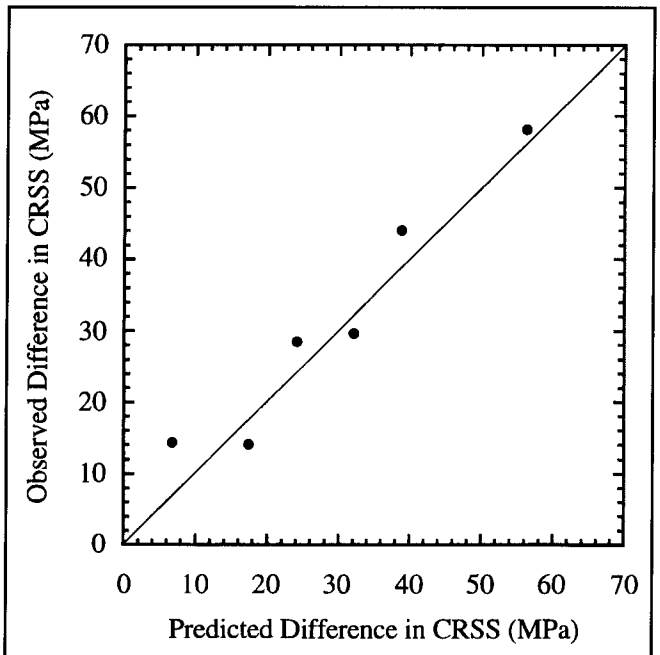

Fig. 5 Comparison between the difference in CRSS predicted using the interfacial strengthening model for sheared precipitates and that observed experimentally for an Al-2.86Cu-2.05Li-0.12Zr alloy (AA2090-T8E41) heat treated at 270 °C. It is assumed that the differences in CRSS between any two samples are attributable to differences in the distribution of T_1 plates, and to isolate the contribution of T_1 phase to yield strength, the experimental and predicted data are compared in terms of the incremental differences in CRSS between successive pairs of samples in the aging sequence.

4.2 Experimental Evaluation

An Al-4Cu-0.05Sn (wt.%) alloy is strengthened exclusively by intermediate θ′ (Al_2Cu) precipitate plates formed on $\{100\}_\alpha$ planes, when aged isothermally at 200 °C. Careful examination of the microstructures of fractured tensile samples [97Nie] has revealed no evidence that the θ′ precipitates in this alloy are sheared during tensile plastic deformation, regardless of the aging condition of the alloy. The Orowan equation might thus be used to calculate the contribution of the θ′ precipitates to the yield stress of the alloy in both underaged and overaged conditions. Experimental values of the increments in CRSS attributable to precipitation in such an alloy can be determined as the difference $(\sigma_y/M - \tau_m)$, where σ_y is the 0.2% yield strength of the alloy, $M = 3.06$ is the Taylor factor for polycrystalline face-centered cubic alloys [70Koc], and τ_m is the contribution of the matrix phase to the CRSS of the alloy. The magnitude of τ_m is typically assumed to be of the order of 10 MPa [76Mon]. In the present analysis, $G = 25$ GPa, $r_0 = b = 0.286$ nm, and $\nu = \frac{1}{3}$. Because samples were heat treated for 24 h at 525 °C to coarsen the grain size, and the concentration of solute Cu in Al is very low in overaged samples, contributions due to solid-solution strengthening and grain-boundary strengthening in overaged samples were assumed to be negligible.

Figure 7(a) shows a comparison of the predicted and measured increments in CRSS for the alloy, which are generally in excellent agreement [97Nie]. The CRSS predicted for underaged samples is slightly lower than the experimental value. However, this discrepancy can likely be attributed to solid-solution strengthening, because the solute Cu concentration in the matrix in underaged samples is expected to be higher than that of peak-aged and overaged samples. Another important observation is that the form of the age-hardening response of the alloy can be accounted for exclusively using the Orowan equation. This again demonstrates that it is not necessary to invoke a transition from dislocation shearing to Orowan looping

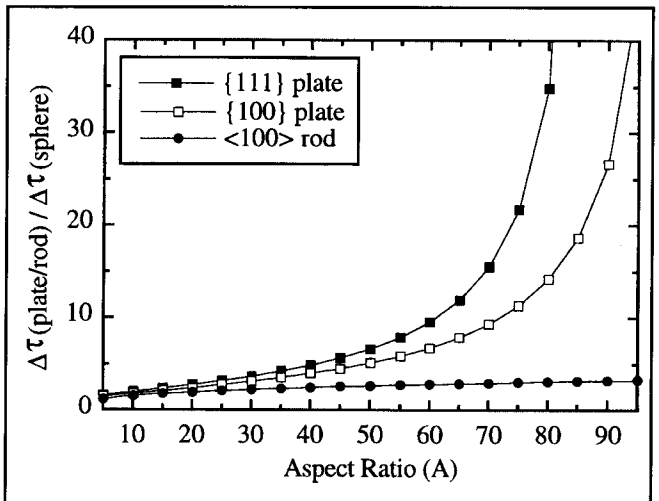

Fig. 6 Variation of ratio $\Delta\tau$(plate/rod)/$\Delta\tau$(sphere) with aspect ratio for Orowan strengthening attributable to $\{111\}_\alpha$ and $\{100\}_\alpha$ precipitate plates and $\langle 100\rangle_\alpha$ precipitate rods (f = 0.05).

to account for the form of the hardening curve. The variation in the effective planar interparticle spacing with aging time is shown in Fig. 7(b), and it is noted that the maximum value in yield strength corresponds approximately to the minimum value in the effective interparticle spacing.

5. Microstructural Modeling and Design

In support of previous work [92Ger], the present analysis of the particle strengthening of Al-Li alloys by coherent δ′ phase demonstrates that the observed form of the age-hardening response can be plausibly modeled assuming a transition from particle shearing to Orowan looping in the classical manner. During the shearing stage, the increase in strength due to the particles is attributed predominantly to the mechanism of order strengthening. However, in assessing the effectiveness of the models applied, it is important to recognize that they depend critically upon key microstructural parameters, such as the precipitate-matrix interfacial energy or the antiphase boundary energy in the precipitate, which are not always known reliably.

In high strength Al alloys, particle strengthening is commonly attributed to distributions of rationally oriented rodlike or, more commonly, plate-shaped particles. The strengthening phases are almost invariably metastable intermediate precipitates that are partially coherent or semicoherent with the matrix phase and, in many cases, the metastable phase equilibria that determine the formation of key strengthening phases have not been examined critically. For many such alloys, it has been established empirically that selected microalloying additions lead to significant changes in precipitation behavior, often with improvements in mechanical properties. The combined addition of Mg and Ag (levels of typically <0.5 wt.%) to the classical Al-4wt.%Cu alloy leads, for example, to the replacement of the metastable tetragonal $\{100\}_\alpha$ precipitate θ′ by a metastable orthorhombic phase Ω of similar composition formed as thin plates on $\{111\}_\alpha$ planes [89Mud]. The resulting microstructure exhibits substantial improvements in strength and thermal stability. However, the role of Mg and Ag in effecting the transition to the Ω phase is yet to be understood.

For strengthening plate-shaped precipitates sheared by dislocations, the present results demonstrate that interfacial (chemical) strengthening can become a major contributor to particle hardening. This is in contrast to spherical particles, where this contribution to strength is generally regarded as negligible. In the case of T_1 plates in Al-Cu-Li alloys, a model of interfacial strengthening that takes account of precipitate shape, orientation, and distribution has been demonstrated to account plausibly for the hardening response of such alloys

Table 2 Equations Defining Increments in CRSS due to Orowan Strengthening for Al Alloys Containing Regular Triangular Arrays of Shear-Resistant Precipitates

Increment in CRSS for Orowan strengthening	Precipitate form
$\Delta\tau = \left\{\frac{Gb}{2\pi\sqrt{1-\nu}}\right\}\left\{\frac{1}{0.931\sqrt{(0.265\pi d_t t_t)/f} - (\pi d_t)/8 - 0.919t_t}\right\}\left\{\ln\frac{1.061t_t}{r_0}\right\}$	$\{111\}_\alpha$ plates
$\Delta\tau = \left\{\frac{Gb}{2\pi\sqrt{1-\nu}}\right\}\left\{\frac{1}{0.931\sqrt{(0.306\pi d_t t_t)/f} - (\pi d_t)/8 - 1.061t_t}\right\}\left\{\ln\frac{1.225t_t}{r_0}\right\}$	$\{100\}_\alpha$ plates
$\Delta\tau = \left\{\frac{Gb}{2\pi\sqrt{1-\nu}}\right\}\left\{\frac{1}{(1.075\sqrt{(0.433\pi)/f} - \sqrt{1.732})d_t}\right\}\left\{\ln\frac{\sqrt{1.732}d_t}{r_0}\right\}$	$\langle 100\rangle_\alpha$ rods

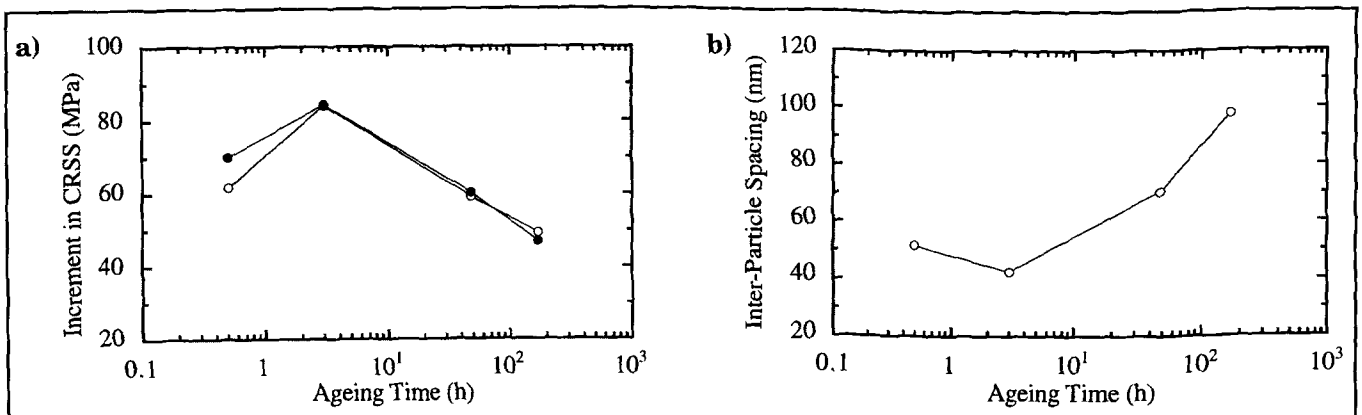

Fig. 7 Variation with aging time of **(a)** increment in CRSS arising from Orowan strengthening, and **(b)** effective interparticle spacing [97Nie]. Alloy Al-4Cu-0.05Sn was aged isothermally at 200 °C. Open circles represent calculated values, and solid circles are observed values.

over the entire aging regime. However, again the reliability of the model is strongly dependent on the values assumed for the particle-matrix interfacial energy and the energy of the particle-matrix interface created when a precipitate is sheared.

For strengthening plate- or rod-shaped precipitates that are resistant to shearing, versions of the Orowan equation, appropriately modified to take account of precipitate shape, orientation, and distribution, are shown to be capable of accounting for observed increments in CRSS. In the case of θ′ plates in Al-Cu-Sn alloy, the appropriate version of the Orowan equation appears to account well for the form of the age-hardening curve, with the maximum in hardness corresponding approximately to a minimum in effective interparticle spacing. Again, it has proven unnecessary to invoke a transition from particle shearing to Orowan looping to allow for the form of the hardness/strength curve as a function of aging time. However, again it is to be recognized that the fit between observed and predicted results depends critically on assumed values of, for example, precipitate-matrix interfacial energy.

Whether particles are sheared or shear resistant, these models confirm experimental observations that high tensile yield strength is associated with microstructures containing a high density of intrinsically strong, plate-shaped precipitates with $\{111\}_\alpha$ or $\{100\}_\alpha$ habit planes and large aspect ratios. As demonstrated in Fig. 2 and 4, the CRSS increment produced by $\{111\}_\alpha$ precipitate plates is comparable to that produced by spherical precipitates, even when the volume fraction of $\{111\}_\alpha$ plates is substantially lower than that of spherical particles. The ultrahigh tensile yield strength (≥700 MPa) observed in Al-Cu-Li-Mg-Ag (X2095) alloy [89Pic] and the high yield strength (550 MPa) of Al-Cu-Li (AA2090) alloys [91Cas] may, for example, be attributable to a uniform distribution of T_1 precipitate plates of large aspect ratio (in the range 40-to-1 to 100-to-1) formed on $\{111\}_\alpha$ planes. It has also been shown that Al-Cu-Mg-Ag alloy, strengthened by the presence of thin plates (typical aspect ratio 30 to 1) of the Ω phase on the $\{111\}_\alpha$ planes, may develop a tensile yield strength exceeding 500 MPa [88Pol]. Furthermore, the well-known high strength of Al-Zn-Mg-Cu alloys (e.g., 7075) is associated with the combined effects of the number density and aspect ratio of precipitate platelets of the phase η′, which also form on the $\{111\}_\alpha$ planes [94Mud]. A remarkably high value of hardness (180 HV) has also been obtained [96Gao] in Al-Cu-Mg-Si alloys by refining the distribution of θ′ precipitate plates formed on the $\{100\}_\alpha$ planes, and complementing this by a fine-scale distribution of $\langle 100\rangle_\alpha$ rods of a quaternary Q phase.

Further improvements in the design of Al alloys for high strength will require an improved understanding of the metastable phase equilibria leading to those intermediate phases forming as plate-shaped products on low-index habit planes. In particular, there needs to be a concerted systematic effort to better understand the role of microalloying additions in determining metastable phase equilibria. For existing alloys strengthened by plate-shaped precipitates, the models outlined in this article suggest that further improvements in strength might be achieved by increasing the number density and/or aspect ratios of the plates. One approach to achieving an increase in plate aspect ratio may lie in the use of microalloying additions, which partition to either matrix or precipitate phase to improve coherency of the precipitate phase in the habit plane.

Cited References

37Kol: A.E. Kolmogorov, *Akad. Nauk. SSSR, IZV, Ser. Mat., 1,* 355 (1937).

39Avr: M. Avrami, *J. Chem Phys., 7,* 1103 (1939).

39Joh: W.A. Johnson and R.F. Mehl, *Trans. AIME, 135,* 416 (1939).

48Oro: E. Orowan, *Symposium on Internal Stresses in Metals and Alloys,* Institute of Metals, London, 451 (1948).

61Lif: I.M. Lifshitz and V.V. Slyozov, *J. Phys. Chem. Solids, 19,* 35 (1961).

61Wag: C. Wagner, *Z. Electrochem., 65,* 581 (1961).

63Fri: J. Friedel, *Electron Microscopy and Strength of Crystals,* G. Thomas and J. Washburn, Ed., Interscience, New York, 605 (1963).

70Koc: U.F. Kocks, "The Relation between Polycrystal Deformation and Single-Crystal Deformation," *Metall. Trans., 1,* 1121-1143 (1970).

73Kel: P.M. Kelly, "The Quantitative Relationship between Microstructure and Properties in Two-Phase Alloys," *Int. Met. Rev., 18,* 31-36 (1973).

75Chr: J.W. Christian, *The Theory of Transformations in Metals and Alloys,* Pergamon Press, Oxford (1975).

76Mon: L.F. Mondolfo, *Aluminium Alloys: Structure and Properties,* Butterworths, London (1976).

84Bau: S.F. Baumann and D.B. Williams, "A New Method for the Determination of the Precipitate-Matrix Interfacial Energy," *Scr. Met., 18,* 611-616 (1984).

85Ard: A.J. Ardell, "Precipitation Hardening," *Metall. Trans. A, 16A,* 2131-2165 (1985).

86Ard: A.J. Ardell, "Precipitation Strengthening: General Considerations," *Encyclopaedia of Materials Science and Engineering,* Vol. 5, M.B. Bever, Ed., Pergamon Press, Oxford, UK, 3882-3887 (1986).

86Cas: W.A. Cassada, G.J. Shiflet, and E.A. Starke, "The Effect of Germanium on the Precipitation and Deformation Behaviour of Al-2Li Alloys," *Acta Metall., 34,* 367-378 (1986).

87Hua: J.C. Huang and A.J. Ardell, "Strengthening Mechanisms Associated with T_1 Particles in Two Al-Li-Cu Alloys," *J. Phys., C3*(9), 373-383 (1987).

88How: J.M. Howe, J. Lee, and A.K. Vasudevan, "Structure and Deformation Behaviour of T_1 Precipitate Plates in an Al-2Li-1Cu Alloy," *Metall. Trans. A, 19,* 2911-2920 (1988).

88Hua: J.C. Huang and A.J. Ardell, "Addition Rules and the Contribution of δ′ Precipitates to Strengthening of Aged Al-Li-Cu Alloys," *Acta Metall., 36,* 2995-3006 (1988).

88Kha: A.G. Khachaturyan, T.F. Lindsey and J.W. Morris, Jr., "Theoretical Investigation of the Precipitation of δ′ in Al-Li," *Metall. Trans. A, 19A,* 249-258 (1988).

88Pol: I.J. Polmear and M.J. Couper, "Design and Development of an Experimental Wrought Aluminium Alloy for Use at Elevated Temperatures," *Metall. Trans. A, 19,* 1027-1035 (1988).

89Emb: J.D. Embury, D.J. Lloyd, and T.R. Ramachandran, "Strengthening Mechanisms in Aluminium Alloys," *Aluminium Alloys: Contemporary Research and Applications,* Treatise on Materials Science and Technology, Vol. 31, A.K. Vasudevan and R.D. Doherty, Ed., Academic Press, New York, NY, 579-601 (1989).

89Mud: B.C. Muddle and I.J. Polmear, "The Precipitate Ω Phase in Al-Cu-Mg-Ag Alloys," *Acta Metall., 37,* 777-789 (1989).

89Pic: J.R. Pickens, F.H. Heubaum, T.J. Langan, and L.S. Kramer, "Al-(4.5-6.3)Cu-1.3Li-0.4Ag-0.4Mg-0.14Zr Alloy Weldalite 049," *Proc. Fifth Int. Conf. on Aluminium-Lithium Alloys,* E.A. Starke and T.H. Sanders, Ed., Mat. and Comp. Eng. Publications, Birmingham, U.K., 1397-1414 (1989).

90Met: *Metals Handbook,* Vol. 2, 10th Ed., ASM International, Materials Park, OH (1990).

91Cas: W.A. Cassada, G.J. Shiflet, and E.A. Starke, "The Effect of Plastic Deformation on Al_2CuLi (T_1) Precipitation," *Metall. Trans. A, 22A,* 299-306 (1991).

91Wag: R. Wagner and R. Kampmann, "Homogeneous Second Phase Precipitation," *Materials Science and Technology: A Comprehensive Treatment,* Vol. 5, R.W. Cahn, P. Haasen, and E.J. Kramer, Ed., VCH, Weinheim, Germany, 213-303 (1991).

92Ger: V. Gerold, H.J. Gudladt, and J. Lendvai, "Microstructure and Deformation Behaviour of Age Hardenable Al-Li Single Crystals," *Phys. Status Solidi (a), 131,* 509-522 (1992).

92Sch: G. Schmitz and P. Haasen, "Decomposition of an Al-Li Alloy—The Early Stages Observed by HREM," *Acta Metall. Mater., 40,* 2209-2217 (1992).

92Tri: K. Trinckauf, J. Pesicka, C. Schlesier, and E. Nembach, "The Effect of the Volume Fraction on Precipitate Coarsening in Nickel-Based Superalloys and Aluminium-Lithium Alloys," *Phys. Status Solidi (a), 131,* 345-355 (1992).

93Hor: E. Hornbogen and E.A. Starke, "Theory Assisted Design of High Strength Low Alloy Aluminium," *Acta Metall. Mater., 41,* 1-16 (1993).

93Rep: B. Reppich, "Particle Strengthening," *Materials Science and Technology: A Comprehensive Treatment,* Vol. 6, R.W. Cahn, P. Haasen, and E.J. Kramer, Ed., VCH, Weinheim, Germany, 311-357 (1993).

94Jeo: S.M. Jeon and J.K. Park, "Transition Behaviour of Deformation Mode from Shearing to Looping in Al-Li Single Crystals," *Philos. Mag. A, 70,* 493-504 (1994).

94Mud: B.C. Muddle, S.P. Ringer, and I.J. Polmear, "High Strength Microalloyed Aluminium Alloys," *Advanced Materials '93, VI / Frontiers in Materials Science and Engineering,* S. Somiya, M. Doyama, and R. Roy., Ed., Elsevier Science B.V., Tokyo, Japan; also in *Trans. Mat. Res. Soc. Jpn., 19B,* 999-1023 (1994).

95Pol: I.J. Polmear, *Light Alloys,* 3rd ed., Edward Arnold, London (1995).

95Sch: C. Schlesier and E. Nembach, "Strengthening of Aluminium-Lithium Alloys by Long-Range Ordered δ′ Precipitates," *Acta Metall. Mater., 43,* 3983-3990 (1995).

96Gao: X. Gao, J.F. Nie, and B.C. Muddle, "High Strength Al-Cu-Mg(-Ag) Alloys with Controlled Si Additions," *Proc. Materials Research 96,* Vol. 1, Institute of Metals and Materials Australasia, Melbourne, Australia, 33-36 (1996).

96Jeo: S.M. Jeon and J.K. Park, "Precipitation Strengthening Behaviour of Al-Li Single Crystals," *Acta Mater., 44,* 1449-1455 (1996).

96Nie: J.F. Nie, B.C. Muddle, and I.J. Polmear, "The Effect of Precipitate Shape and Orientation on Dispersion Strengthening in High Strength Aluminium Alloys," *Mater. Sci. Forum, 217-222,* 1257-1262 (1996).

97Nem: E. Nembach, *Particle Strengthening of Metals and Alloys,* John Wiley & Sons, Inc., New York (1997).

97Nie: J.F. Nie and B.C. Muddle, unpublished work (1997).

97Nob: B. Noble, S.J. Harris, and K. Dinsdale, "Microstructural Stability of Binary Al-Li Alloys at Low Temperatures," *Acta Mater., 45,* 2069-2078 (1997).